Journal of New Materials for Electrochemical Systems 20, 123-127 (2017)
© J. New Mat. Electrochem. Systems

A Potential Hydrogen Source from Milled Silicon Powder Activated by Lithium and Aluminum Chloride

Tianchu Yin, Hongwei ShenTu, Chengqiao Xi, Xin Chen, Wenzhen Zou and Meiqiang Fan

Department of Materials Science and Engineering, China Jiliang University, Hangzhou 310018, P R China

Received: June 04, 2017, Accepted: July 11, 2017, Available online: July 28, 2017

Abstract: *A potential hydrogen source generated from milled Li-Si-$AlCl_3$ composite was evaluated in this paper. The composite exhibits good hydrogen generation performance in water at 313–343 K, whereas pure silicon powder cannot continuously react with water under similar conditions. The hydrogen yield reaches 1300 mL hydrogen/g within 20 min, and the highest hydrogen generation rate is higher than 1200 mL hydrogen/g min within the first minute of hydrolysis. The hydrogen generation performance increases with increasing concentrations of lithium and aluminum chloride. Microstructure analysis indicates that silicon activity increases due to decreased particle size and distribution of lithium and aluminum chloride into silicon matrix during milling. The hydrolysis of the additives generates heat and alkaline hydrolysis byproducts, thereby stimulating the hydrolysis rate of silicon in the micro area. Therefore, the hydrolysis of silicon in water may act as a potential hydrogen source for portable micro fuel cells.*

Keywords: Li-Si-$AlCl_3$ composite, hydrolysis, hydrogen generation

1. INTRODUCTION

Hydrogen is a good alternative fuel to hydrocarbons because of its high chemical energy per unit mass and pollution-free combustion product. However, storage and transportation of hydrogen remain challenging because of it possesses low density and should be heavily compressed in steel containers [1, 2].

Alternative energy storage methods should be developed for large-scale hydrogen application in vehicles and portable apparatus [3–6]. Chemical hydrogen storage materials can generate hydrogen through chemical reactions at room temperatures [7–9]. In the past 30 years, numerous chemical hydrogen storage materials have been developed as composition design, catalyst, and hydrogen generator; these materials include metals, borohydrides, and metal hydrides [10–12]. Silicon is a promising material because of its high theoretical gravimetric hydrogen storage value of 14 wt%, low cost, and abundance. Silicon can react with water to generate hydrogen at mild temperature, but the reaction is severely terminated by the formation of dense silica film on the silicon surface [13]. In this regard, methods for removing the oxide layer should be develop to achieve sustainable reaction of silicon and water [14, 15]. Generally, nanosilicon exhibits improve hydrolysis performance than micro silicon powders. Erogbogbo [16] synthesized silicon particles with 10 nm diameter and observed that their hydrogen generation rate in water is 1000 times faster than that of 325 mesh silicon powders. Foorde [17] reported that milled 325 mesh silicon can constantly react with water to generate hydrogen; however, the hydrogen yield is lower than 70% due to the effect of the silica byproduct from hydrolysis. Alkaline solutions, such as sodium or potassium hydroxide, can also be used to accelerate the hydrolysis of silicon by removing the passivating oxide layer [18, 19]. The reaction rate of silicon and hydroxides is higher than those of silicon or nanosilicon with water. The different reactions of silicon with water or alkaline solutions are typically expressed in Equations 1, 2, and 3 [20, 21].

$$\mathrm{Si(cr)+4H_2O(l) \rightarrow Si(OH)_4+2H_2(g)} \qquad \text{Eq.1}$$

$$\mathrm{Si(cr)+2H_2O(l) \rightarrow SiO_2+2H_2(g)} \qquad \text{Eq.2}$$

$$\mathrm{Si(cr)+2OH^-(aq) +2H_2O(l) \rightarrow SiO_2(OH)_2^{2-}+2H_2(g)} \qquad \text{Eq.3}$$

In Equation 3, the hydroxide behaves as a catalyst and as a stoichiometric reagent. The concentration and volume of the hydroxide considerably affect the reaction rate of silicon. Seidel observed that the reaction rate of silicon increased with increasing hydroxide concentration and solution volume when using 10–60 wt% potassium hydroxide solutions [21]. Brack reported that 80% of

---

*To whom correspondence should be addressed: Email: fanmeiqiang@126.com the theoretical hydrogen yield was achieved from the reaction of 325 mesh silicon powder and 20 wt% sodium hydroxide solution at 323 K [22]. However, strong alkaline solutions are potentially harmful for common users when silicon is used for hydrogen generation.

In our previous work, milled lithium aluminum composite can rapidly react with water at 298 K and achieve 100% of the theoretical hydrogen yield [23]. The addition of lithium can ruin alumina layer and stimulate the sustainable hydrolysis of aluminum. So milled lithium silicon composites may also react with water under mild conditions. To our knowledge, the composition design and relative hydrogen generation performance of lithium silicon composites have not been reported yet. In the present work, we prepared lithium silicon composite through milling method. The hydrogen generation performance and the effect of lithium or aluminum chloride on the composite were investigated. This work aims to optimize silicon composition design and present relative mechanisms.

2. EXPERIMENTAL

2.1. Sample preparation

Silicon powder (99.9% purity, particle size of approximately 10 µm), lithium plate (99% purity), and aluminum chloride powder (99% purity, particle size of below 100 µm) were obtained from Mike reagent company in Hangzhou City, China. The powders were weighed, sealed in 50 mL stainless steel jars, and added with stainless steel balls at a ball-to-mixture weight ratio of 26:1. The powders were milled at 300 r/min for 10 h in a planetary ball miller from Nanjing University in P. R China. Aluminum chloride salt can prevent the agglomeration of lithium and silicon during milling and accelerate the hydrolysis reaction of silicon and water. Different mass ratios of lithium-to-silicon and aluminum chloride-to-silicon were used for composition design.

2.2. Evaluation of hydrogen generation performance

Hydrogen generation experiments were carried out in a sealed reactor attached to a condenser and a graduated cylinder at 298 K and 1 atm. The mass ratio of mixture-to-water was set to 1:20, and the hydrolysis temperature was 323 K unless otherwise stated.

2.3. Microstructure analysis

Powder X-ray diffraction patterns were collected on an X-ray diffractometer (Thermo Arl X’tra, Switzerland) by using Cu Ka radiation. The samples were mounted as powders on glass tape. Data were collected over the 2θ range of 20°–80°, with a step size of 5°/min. Scanning electron microscopy observations were conducted on a Jsm-5610lv (Jeol Co.) equipped with an Inca energy-dispersive X-ray spectrometer.

3. RESULTS AND DISCUSSION

3.1. Hydrogen generation performance

Figure 1 shows the hydrogen generation curves of the milled Li–Si–$AlCl_3$ composite with different Li/Si mass ratios. Hydrogen was not collected from the reaction of silicon and water. This finding indicates that silicon powder exhibits high stability in water. Hydrogen was instantly generated from the reaction of silicon powder and 1 M lithium hydroxide solution. Only 1190 mL hydrogen/g or 68% of the hydrogen yield was achieved within 20 min. Meanwhile, the Li (10 wt%)–Si (85 wt%)–$AlCl_3$ (5 wt%) composite exhibited 1382 mL hydrogen/g or 79% of the hydrogen yield within 20 min under similar conditions. The Li (15 wt%)–Si (80 wt%)–$AlCl_3$ (5 wt%) composite possessed 1482 mL hydrogen/g or 90% of the hydrogen yield within 20 min. The Li (20 wt%)–Si (75 wt%)–$AlCl_3$ (5 wt%) composite has 1571 mL hydrogen/g or 95% of hydrogen yield within 20 min. The Li–Si–$AlCl_3$ composite exhibited higher hydrogen generation performance than silicon in water or alkaline solution.

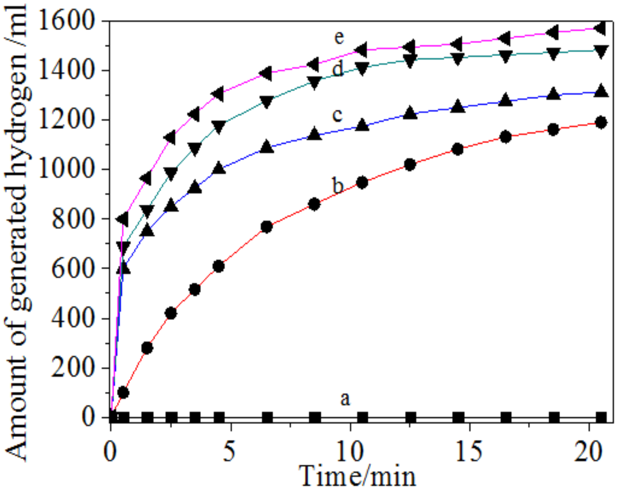

Figure 1. Hydrogen generation curves of milled Li-Si-$AlCl_3$ composite with different Li/Si mass ratios. a, pure silicon powder in water; b, pure silicon powder in 1 M 50 ml LiOH solution; c, Li (10 wt%)-Si (85 wt%)- $AlCl_3$ (5 wt%) composite in water; d, Li (15 wt%)-Si (80 wt%)- $AlCl_3$ (5 wt%) composite in water; e, Li (20 wt%)-Si (75 wt%)- $AlCl_3$ (5 wt%) composite in water

The highest hydrogen generation rates of Li (10 wt%)–Si (85 wt%)–$AlCl_3$ (5 wt%) composite, Li (15 wt%)–Si (80 wt%)–$AlCl_3$ (5 wt%) composite, and Li (20 wt%)–Si (75 wt%)–$AlCl_3$ (5 wt%) composite were 1200, 1375, and 1600 mL hydrogen/g min, respectively. The hydrogen generation performance improved with increasing lithium content in the composite.

Aluminum chloride can prevent the blocking of silicon powder and acids present in water. The concentration of aluminum chloride may significantly affect the hydrogen generation performance of silicon powder. Figure 2 shows the hydrogen generation curves of the milled Li–Si–$AlCl_3$ composites with different aluminum chloride concentrations. The mass ratio of lithium-to-silicon was fixed according to Li (15 wt%)–Si (80 wt%)–$AlCl_3$ (5 wt%) composite. The lithium silicon composite without $AlCl_3$ generated 1360 mL hydrogen/g or 78% of the hydrogen yield within 20 min. The lithium silicon composite with 5 wt% $AlCl_3$ exhibited 1482 mL hydrogen/g or 90% of the hydrogen yield within 20 min. The composite with 10 wt% $AlCl_3$ generated 1530 mL hydrogen/g or 98% of the hydrogen yield. The highest hydrogen generation rates of lithium silicon composite without $AlCl_3$, 5 wt% $AlCl_3$, and 10 wt% $AlCl_3$were 1120, 1375, and 1540 mL hydrogen/g min, respectively.

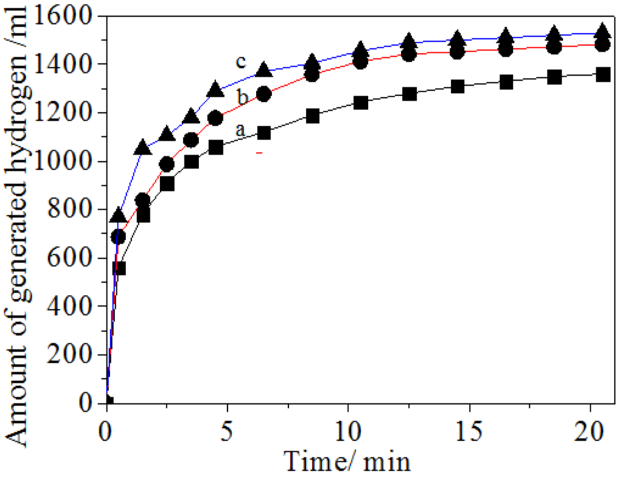

Figure 2. Hydrogen generation curves of milled Li-Si-$AlCl_3$ composite with different $AlCl_3$ concentrations. a, Without $AlCl_3$; b, 5 wt% $AlCl_3$; c, 10 wt% $AlCl_3$.

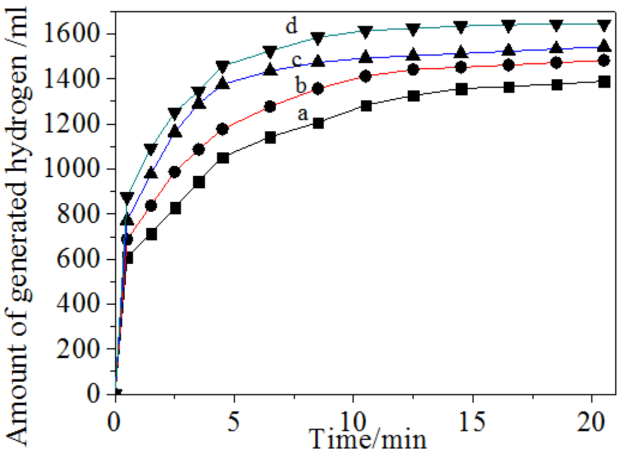

Figure 3. Hydrogen generation curves of milled Li (10 wt%)-Si (85 wt%)- $AlCl_3$ (5 wt%) composite at different temperatures. a, 313 K; b, 323 K; c, 333 K; d, 343 K.

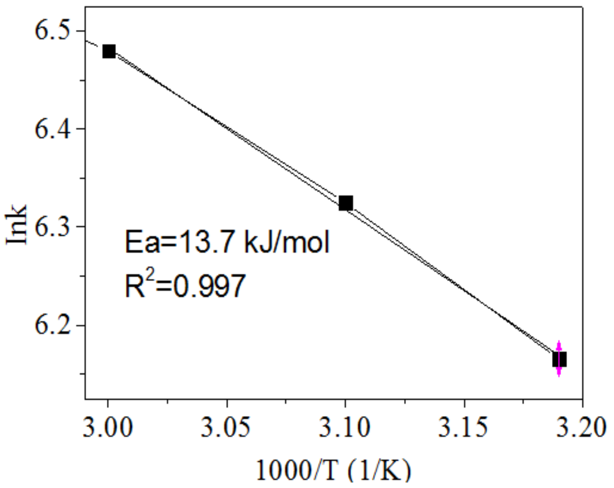

Figure 4. Relationship between lnk and 1/T. k is the hydrogen generation rate of milled Li (10 wt%)-Si (85 wt%)- $AlCl_3$ (5 wt%) composite and water, T is hydrolysis temperature.

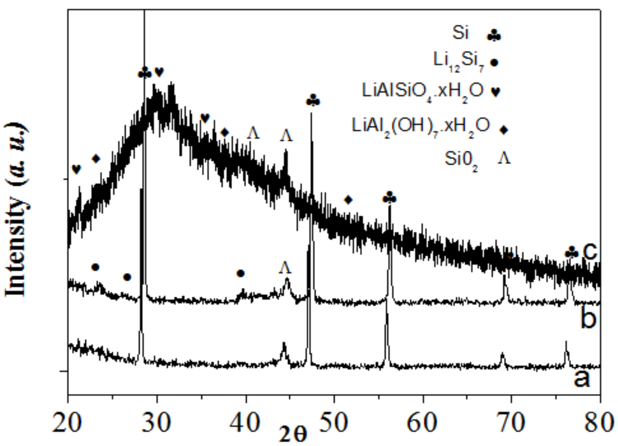

Figure 5. XRD patterns of Si (a), milled Li-Si-$AlCl_3$ composite before (b) and after hydrolysis (c).

The hydrogen generation performance improved with increasing aluminum chloride content in the composite. However, the added $AlCl_3$ cannot react with water to generate hydrogen; therefore, the $AlCl_3$ content in the composite should be limited.

Temperature is an important parameter that affects silicon hydrolysis. Figure 3 shows the hydrogen generation curves of the milled Li (15 wt%)–Si (80 wt%)–$AlCl_3$ (5 wt%) composite at different temperatures. The composite generated 1390 mL hydrogen/g (or 84% of hydrogen yield) at 313 K, 1482 mL hydrogen/g (or 90% of hydrogen yield) at 323 K, 1543 mL hydrogen/g (or 93% of hydrogen yield) at 333 K, and 1644 mL hydrogen/g (or 99% of hydrogen yield) at 343 K within 20 min. The hydrogen yield of the composite increased with increasing hydrolysis temperature. The highest hydrogen generation rate also presented similar trend to the increase in hydrolysis temperature. In the beginning of hydrolysis, the composite generated 1218 mL hydrogen/min g at 313 K, 1375 mL hydrogen/min g at 323 K, 1542 mL hydrogen/min g at 333 K, and 1750 mL hydrogen/min g at 343 K. Based on Arrhenius equation, the highest hydrogen generation rate can be used to calculate activation energy.

$$k = Ae^{-E\alpha/RT} \rightarrow In\,k = In\,\mathrm{A} - \mathrm{E_a}/RT \qquad \text{Eq.4}$$

Where k is highest hydrogen generation rate, T is the hydrolysis temperature, *E*a is the activation energy, and R is the molar gas constant. The relationship between ln k and 1/T can be linearly fitted in Figure 4. From the slope value at Figure 4, the activation energy (*E*a) was calculated to be 13.7 kJ/mol, which is lower than that of silicon (66.9 kJ/mol) [24]. Hence, the addition of lithium and aluminum chloride improved the hydrogen generation performance of silicon in water.

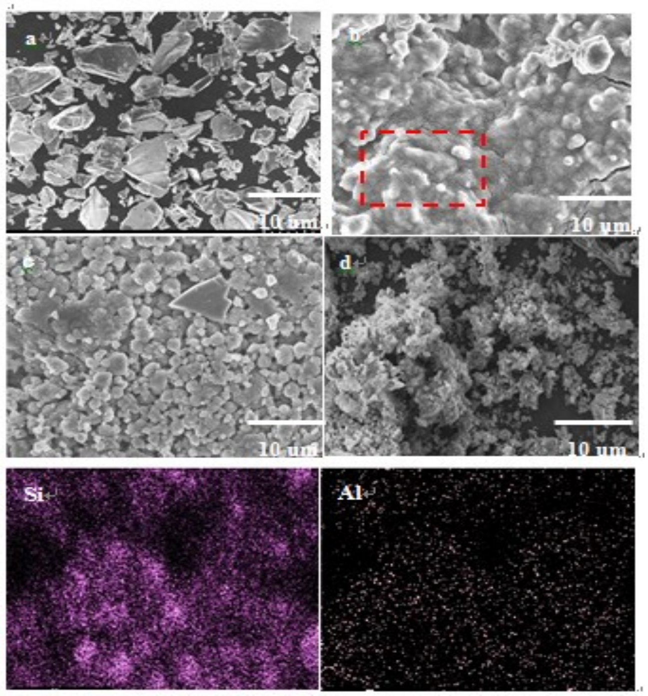

Figure 6. Morphologies and EDS of Si (a), milled Li (10 wt%)-Si (80 wt%)- $AlCl_3$ (10 wt%) composite (b); milled Li (15 wt%)-Si (80 wt%)- $AlCl_3$ (5 wt%) composite (c); milled Li (10 wt%)-Si (80 wt%)- $AlCl_3$ (10 wt%) composite after hydrolysis (d).

3.2. Material microstructure

Figure 5 shows the XRD patterns of Si (a), milled Li–Si–$AlCl_3$ composite before (b) and after hydrolysis (c). The XRD patterns of silicon powder show characteristic peaks (PDF card 65-1060) at 28.6°, 47.3°, 56.1°, 69.1°, and 76.4°. The XRD patterns of the milled Li–Si–$AlCl_3$ composite show new peaks for $Li_{12}Si_7$, except peaks for silicon. The results indicate that occurrence of alloying of lithium and silicon during milling. The formation of lithium silicon alloy decreased the size of the silicon particles. Therefore, the silicon peaks in the XRD patterns of the Li–Si–$AlCl_3$ composite are wider than those of silicon powder. The peaks for lithium silicon alloy and silicon disappeared, and new peaks for SiO_2 (PDF card 14-0654), $LiAlSiO_4.xH_2O$ (PDF 27-1211), and $LiAl_2(OH)_7.xH_2O$ (PDF 31-0704) were observed in the XRD patterns of the Li–Si–$AlCl_3$ composite after hydrolysis. These results are consistent with the hydrogen generation performance in Figures 1–4.

Figure 6 shows the morphologies of Si and milled Li–Si–$AlCl_3$ composite before and after hydrolysis. The silicon powder presents irregular plates, with particle size ranging from 1 µm to 10 µm. After milling with lithium and aluminum chloride, the silicon shape changed. Numerous blocks and nanofibers were observed in the morphologies of the Li (10 wt%)–Si (80 wt%)–$AlCl_3$ (10 wt%) composite and Li (15 wt%)–Si (80 wt%)–$AlCl_3$ (5 wt%) composite. Morphology analysis and EDS results identified the nanofibers as aluminum chloride. The uniform distribution of aluminum chloride in the silicon matrix was further confirmed from the element mapping results in Figure 6. After hydrolysis, several loose and irregular cotton-shaped solids accumulated, and their sizes range in several micrometers.

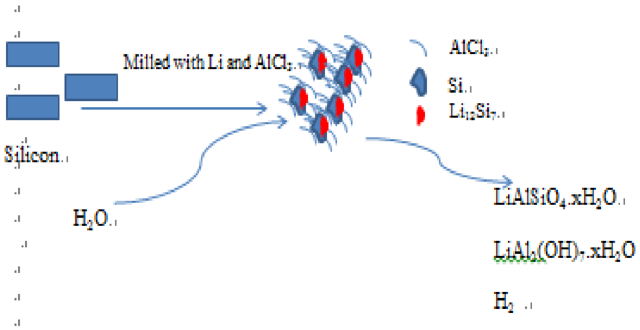

Figure 7. Activation and hydrolysis of Li-Si-$AlCl_3$ composite.

3.3. Activation and hydrolysis mechanism

From the hydrogen generation performance in Figure 1-3, the concentrations of lithium and aluminum chloride have great effects to improve the hydrogen generation performance of silicon. It can be easily deduced that the activation of silicon is firstly based on its particle size decrease and the distribution of lithium and aluminum chloride into silicon matrix in the milling process in Figure 7. The particle size of Li-Si-$AlCl_3$ composite can be explained to the formation of lithium silicon alloy and the prevention of aluminum chloride against the block of Si-Si and Li-Li.

In addition, the activity of silicon may be improved due to the alkaline solution from lithium hydrolysis. Silicon hydrolysis is categorized into three stages (Figure 7). In the first stage, the added lithium and aluminum chloride exhibit high activity and rapidly react with water, as shown in Equations 5–8 [23, 25]. In the second stage, hydrolysis byproducts, namely, lithium hydroxide and aluminum hydroxide, lead to alkaline solution on the silicon surface; this alkaline solution catalyzes silicon hydrolysis. Large amounts of hydrogen are generated in this stage according to Equation 3. Lithium hydrolysis releases a large amount of heat and the hydrolysis byproduct lithium hydroxide, which is limited in a micro area and simulates the hydrolysis rate of silicon (Figures 1 and 6). Finally, in the third stage, the hydrolysis byproducts, namely, silica, lithium hydroxide, and aluminum oxide, combine with water to generate solid-state hydrate particles (as shown in Equations 9 and 10).

First stage:

$$2Li+2H_2O \rightarrow 2LiOH+H_2 \qquad \text{Eq.5}$$

$$AlCl_3+H_2O \rightarrow AlOHCl_2+HCl \qquad \text{Eq.6}$$

$$AlOHCl_2+H_2O \rightarrow Al(OH)_2Cl+HCl \qquad \text{Eq.7}$$

$$Al(OH)_2Cl+H_2O \rightarrow Al(OH)_3+HCl \qquad \text{Eq.8}$$

Second stage:

$$Si(cr)+ 2OH^-(aq) +2H_2O(l) \rightarrow SiO_2(OH)_2^{2-}+2H_2(g) \qquad \text{Eq.3}$$

Third stage:

$$LiOH+ Al(OH)_3+ SiO_2 \rightarrow LiAlSiO_4.2H_2O \qquad \text{Eq.9}$$

$$LiOH+ 2Al(OH)_3 + 2H_2O \rightarrow LiAl_2(OH)_7.2H_2O \qquad \text{Eq.10}$$

4. CONCLUSION

Li–Si–$AlCl_3$ composite was prepared through milling, and its hydrogen generation performance was evaluated. The results of the analysis are summarized as follows:

1) The Li–Si–$AlCl_3$ composite exhibits good hydrogen generation performance in water at mild temperatures; the performance improves with increasing concentration of lithium and aluminum chloride. The hydrogen yield reaches 1300 mL hydrogen/g within 20 min. The highest hydrogen generation rate is higher than 1200 mL hydrogen/g min within the first minute of hydrolysis.
2) The increase in the activity of silicon is due to the following factors: (a) the particle size decreases, and lithium and aluminum chloride are distributed in the silicon matrix during milling. (b) The alkaline hydrolysis byproducts and large amount of heat generated through hydrolysis of lithium and aluminum chloride stimulate the hydrolysis of silicon in the micro area.

Therefore, the milled Li–Si–$AlCl_3$ composite may be a potential hydrogen source for portable microfuel cells in the future.

5. ACKNOWLEDGMENTS

This work was financially supported by the Scientific Research Foundation for the Returned Scholars, postdoctoral support of P. R China (2015M581910), postdoctoral preferential support of Zhejiang province (BSH1502029), the National Science Foundation of China (Project No. 51501175).

REFERENCE

[1] Schlapbach L., Zuttel A., Nature, 414, 353 (2001).
[2] Gerboni R., Salvador E., Energy, 34, 2223 (2009).
[3] Yang J., Sudik A., Wolverton C., Siegel J.S., Chem. Soc. Rev., 39, 656 (2010).
[4] Sakintuna B., Lamari-Darkrim F., Hirscher M., Int. J. Hydrogen Energy, 32, 1121 (2007).
[5] Matsunaga T., Buchter F., Miwa K., Towata K., Zuttel A., Renewable Energy, 33, 193 (2008).
[6] Garcia R.S., Weisser D., Renewable Energy, 31, 2296 (2006).
[7] Wang Y., Shen Y., Qi K. Z., Cao Z. Q., Zhang K., Renewable Energy, 89, 285 (2016).
[8] Fan M. Q., Liu S., Sun W. Q., Fei Y., Renewable Energy, 46, 203 (2012).
[9] Liang J., Gao J., Miao N. N., Chai Y. J., Wang N., Energy, 113, 282 (2016).
[10]Shafirovich E., Diakov V., Varma A., Combust Flame, 144, 415 (2006).
[11]Liu BH, Li Z P., J. Power sources, 187, 527 (2009).
[12]Choi B., Panthi D., Nakoji M., Kabutomori T., Tsutsumi K., Int. J. Hydrogen Energy, 47, 6197 (2015).
[13]Philipsen H. G. G., OZanam F., Allongue P., Kelly J. J. Chazalviel J. N., Surface Science, 644, 180 (2016).
[14]Palik, E.D., Gray, H.F., Klein, P.B., J. Electrochem. Soc., 130, 956 (1983).
[15]Philipsen, H.G.G., Kelly, J.J., Electrochim. Acta, 54, 3526 (2009).
[16]Erogbogbo, F., Lin, T., Tucciarone, P.M., et al., Nano Lett., 13, 451 (2013).
[17]Foord, J.S., Ashraf, S., Preparation of silicon for fast generation of hydrogen through reaction with water, WO, 2011/058317
[18]S Shah, I., Koekkoe J.J., Enckevort W.J.P., Vlieg, E., Cryst. Growth Des., 9, 4315 (2009).
[19]Dai, F., Zai, J., Yi, R., Nat. Commun., 5, 3605 (2014).
[20]Tichapondwa, S.M., Focke, W.W., Del Fabbro, O., J. Energ. Mater., 29, 326 (2011).
[21]Seidel, H., Csepregi, L., Heuberger, A., and Baumgartel, H., J. Electrochem. Soc., 137, 3612 (1990).
[22]Brack, P., Dann, S.E., Wijayantha, K.G.U., Energy Sci. Eng., 3, 535 (2015).
[23]Fan M. Q., Sun L. X, XU F., Int. J. Hydrogen energy, 36, 9791 (2011).
[24]Doremus R. H., J. Phys. Chem., 80, 1773 (1976).
[25]Benschoten J. E. V., Edzwald J. K., Wter Rearch, 24, 1519 (1990).